Supplementary Information

for

Electro-nucleation of water nano-droplets in No Man's Land to fault-free ice I*c*

Prithwish K. Nandi[1*+†], Christian J. Burnham [+] and Niall J. English [*+]

[+] *School of Chemical and Bioprocess Engineering, University College Dublin, Belfield, Dublin 4, Ireland*

[†]*Irish Centre for High-End Computing, Grand Canal Quay, Dublin 2, Ireland*

(a) Distribution of intrinsic electric fields

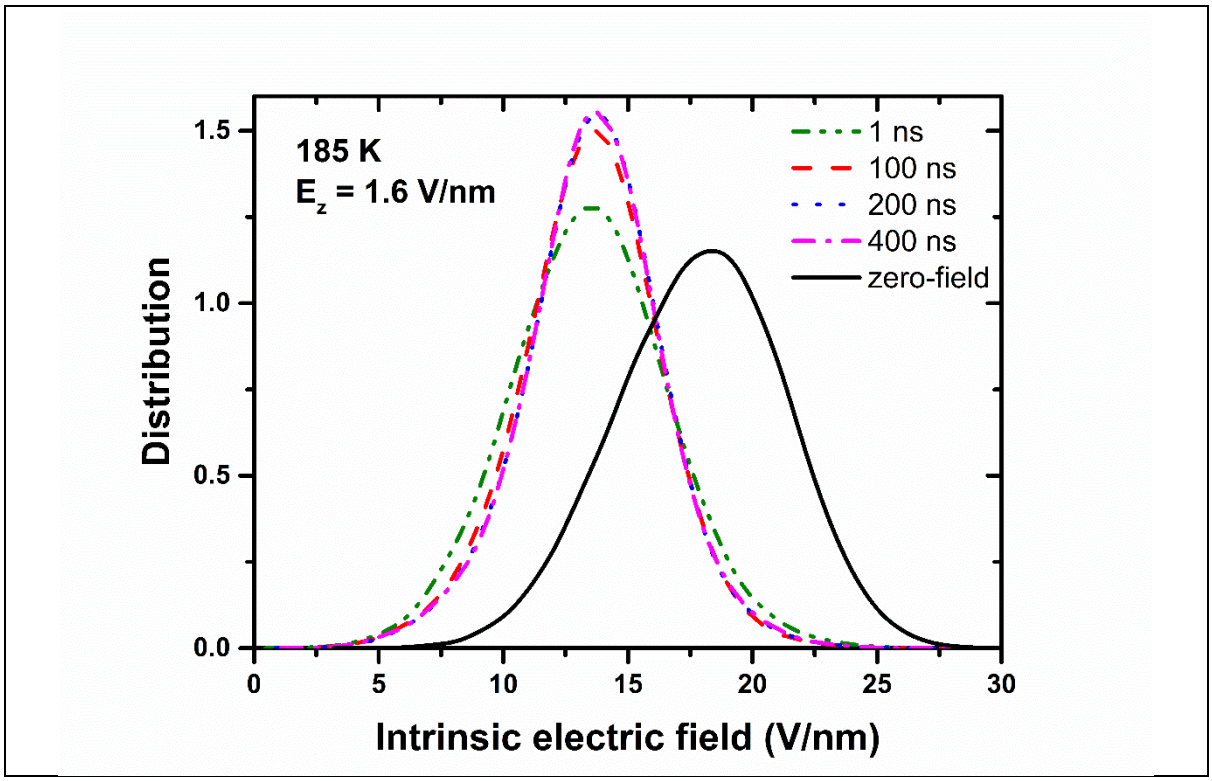

Figure S1. Probability distribution of the intrinsic electric field, *i.e.*, that experienced by a molecule due to all others in the system, under zero-field conditions and also in a 1.6 V/nm field at 185 K at various times (as a typical example). Here, the Coulombic forces were evaluated on each charge site without any cut-off whatsoever from other molecules (excluding the force from the external field), via real-space Coulomb's law, from Smooth-Particle-Mesh-Ewald-propagated MD, and **E** at each such site *i* defined as $\mathbf{f}_i / q_i$, with its magnitude then taken.

* Corresponding authors: prithwish.nandi@ichec.ie, niall.english@ucd.ie, Tel: +353-1-7161646 - NE, +353-1-5241608 (ext. 22) - PN, Fax: +353-1-7161177 - NE

(b) Further comments on applied-field intensities, and justification of 0.2 - 2.5 V/nm range used

As mentioned in the main text, in the physical system of the present study, covalent bonds are mechanically prevented from rupture. Therefore, even for very large fields of ~2-5 V/nm (where external forces are clearly often a deal larger than 15-20% of the intermolecular, regular intrinsic-system forces, and non-linear effects overtly large) water molecules would not exhibit dissociation; clearly, however, this would happen in Nature. Although Saitta and co-workers have pioneered recently very interesting picosecond-scale non-equilibrium *ab initio* MD on water break-up in such very large-magnitude fields, in various environments,[S1] these break-up events were not observed below ~2-5 V/nm, due to necessarily very short timescales. In any event, in the present study, water break-up, in terms of dissociation of chemical bonding would not happen even such very large external fields, although we do not pursue NE-MD with fields larger than 2.5 V/nm, so as to keep external-field forces[15] at less than ~18% of intrinsic-system ones.

A further motivation to adhere to the general 0.2 - 2.5 V/nm external-field intensity range, apart from the main text mentioning a phase-transition 'control' threshold of ~1.5 V/nm found previously for hydrate nano-clusters[25] and being in the general region of external-field forces straddling 10% of intrinsic ones, lies in the fact that the general region of ~0.2-0.5 V/nm is considered by many workers, with a very good deal of supporting evidence[15], to represent the cusp of a linear-to-non-linear transition in the system-response régime, in terms of non-equilibrium MD 'driving' system translational and rotational effects. Naturally, this depends on the precise property being considered to gauge system response[15]. In any event, the range of 0.2 - 2.5 V/nm provides a compromise between being able to witness phase-transition kinetics and structuring effects in the linear and mildly non-linear régime over nanosecond time scales straddling the previously-identified phase-transition-effect threshold of ~1.5 V/nm for hydrate nano-clusters[25] together with avoiding excessively large field intensities with strong and pronounced non-linear system response (above around 2.5 V/nm), which would certainly be expected to lead to some probable water molecular-dissociation events over nanosecond time scales[S1] if the system were not composed of rigid TIP4P/2005 water molecules.

More widely, in previous MD simulations of bulk-water electro-freezing[15-22], substantially large external-field strengths have been used. For instance, Svishchev and Kusalik used a value of 5 V/nm in their studies of electro-crystallisation [16,17], whilst Radhakrishnan and Trout used a value of 10 V/nm [18], and, recently, Luedtke *et al.*[39] have used field strengths up to 2 V/nm, and shown that electro-crystallisation in formamide is achieved for larger fields. Indeed, a knowledgeable discussion on the rather common occurrence of external field strengths of up to several volts per nanometre has also been provided by Luedtke *et al.*[39] where they mentioned correctly that the field strength at the tip of the Taylor cone of an electro-spray device, or in the high-curvature region of a dielectric/ionic mixture-liquid droplet could easily experience external-field strengths of the order of up to several volts/nanometre.

In order to identify the critical external-field 'threshold' strength required to observe field-induced shape elongation, and subsequent electro-crystallisation, simulations at field strengths of 0.2 and 0.5 V/nm indicate the development of aspherical 'bulging' of the initially spherically droplet within 1 μs, suggesting probable further elongation and further crystallisation upon extending simulations over multiple microseconds at 0.2 V/nm, for all three temperatures studied. In 0.5 V/nm fields, we observe characteristic water-droplet elongation and the initial signatures of nucleation centres for 185 and 200 K. For the 0.8 V/nm case, full nucleation occurs at 185 K. However, at 150 K, although shape elongation of the droplet is observed, no nucleation occurred by the end of the 1 μs simulation. Nucleation at 150 K is seen in 1.2 V/nm fields near the end of the 1 μs simulation. A brief summary of shape transformation and nucleation observed for various conditions is presented below (Table S1).

S1. Saitta, A. M.; Saija, F. Miller experiments in atomistic computer simulations. *Proc. Natl. Acad. Sci. U. S. A.*, **2014**, *111*, 13768.

Table S1: Field-strength and temperature effects on morphology deformation and nucleation

	T (K)	0.2 V/nm	0.5 V/nm	0.8 V/nm	1.2 V/nm	1.6 V/nm	2 V/nm	2.5 V/nm
Shape elongation	150	No	No	Yes	Yes	Yes	Yes	yes
	185	Slight aspherical bulging	Yes	Yes	Yes	Yes	Yes	Yes
	200	Slight aspherical bulging	Yes	Yes	Yes	Yes	Yes	Yes
Nucleation	150	No	No	No	Initial nucleation centres observed	Partial	Partial	Partial
	185	Not achieved within 1 µs	Initial nucleation centres observed	Yes	Yes	Yes	Yes	Yes
	200	Not achieved within 1 µs	Initial nucleation centres observed	Yes	Yes	Yes	Yes	Yes

(c) Dipolar Distribution

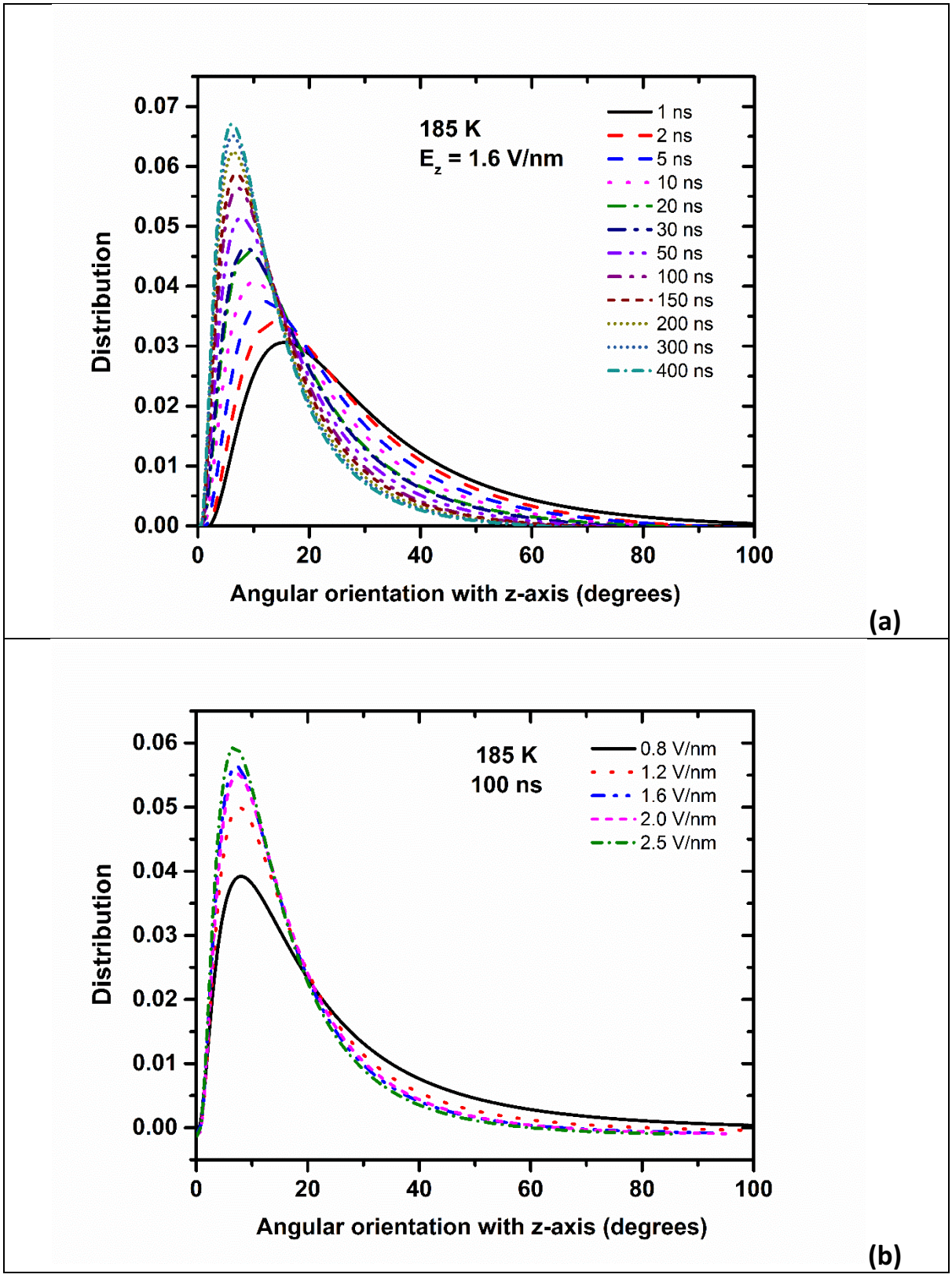

Figure S2: Distribution of molecules' dipolar orientation relative to the external-field direction (the laboratory *z*-axis). In (a), as a typical example, reorientation is shown as a function of simulation time at 1.6 V/nm field at 185 K, whilst (b) depicts this at after 100 ns for increasing field strengths.

(d) Aspect ratios

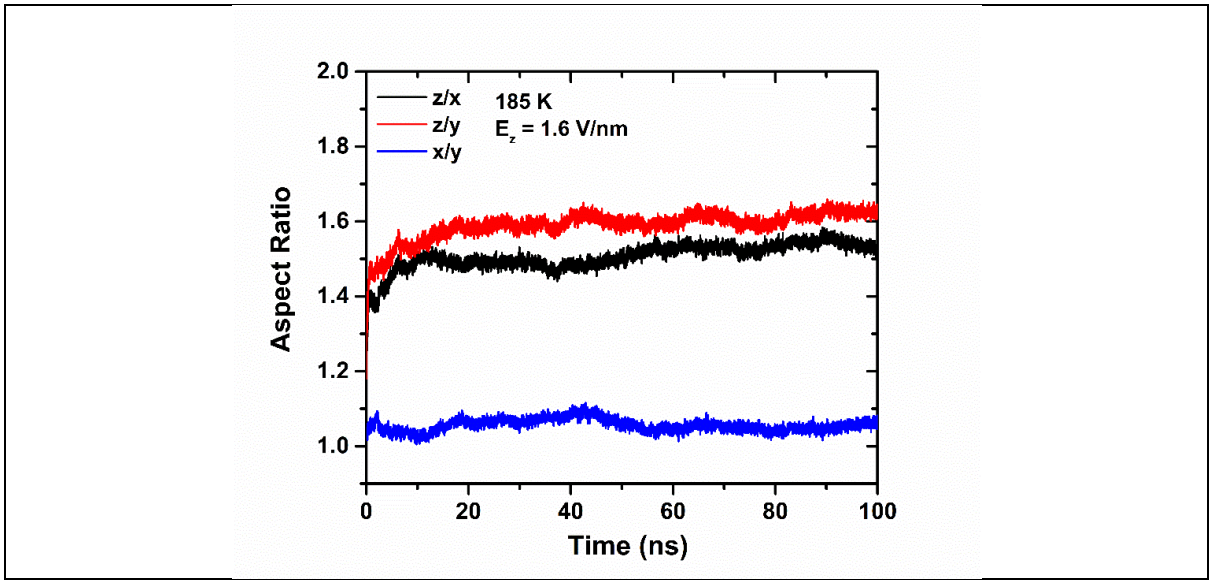

Figure S3*(a)*: *z*/*x*, *z*/*y* and *x*/*y* aspect ratios, underscoring field-mediated *z*-axis elongation; 185 K and 1.6 V/nm is shown here as a typical (and dramatic) example. The aspect ratio is defined in terms of laboratory-axis directional length ratios, where the directional length is gauged from the average of the 2% most extreme coordinate values at each end defining the length along of a particular direction; here, this is essentially restricted to surface molecules, where there are at least two other molecules within 0.35 nm distance. Changing the 'end-definition' threshold between 1 and 5% led to no real change in the aspect ratios.

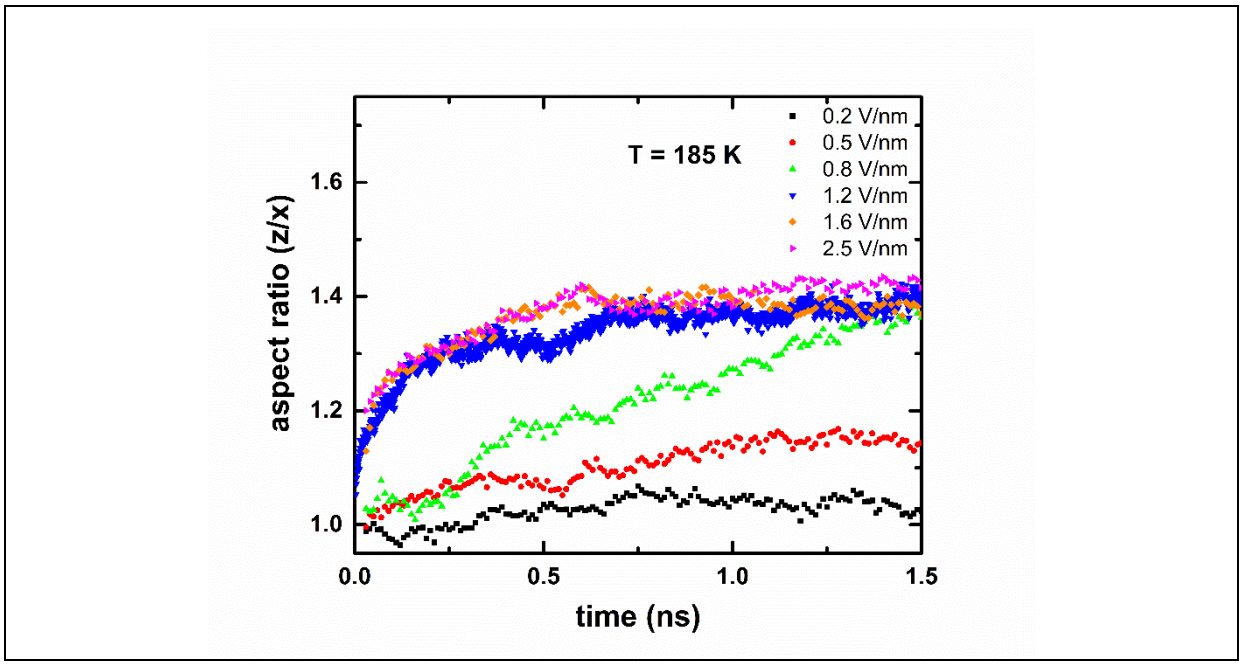

Figure S3(b): *z*/*x* aspect ratio, underscoring field-mediated *z*-axis elongation at 185 K for field intensities varying from 0.2 -2.5 V/nm. Clearly, the onset of shape elongation scales with external-field intensity, suggesting that for observation of similar elongation at much lower field strengths relevant to naturally-occurring static fields in the atmosphere (10^3 – 10^5 V/m),[28,29] simulations need to be run over timescales of the order of a millisecond or longer, which are not yet routinely-accessible with modern-day supercomputers.

(e) Moment-of-Inertia Eigenvalues:

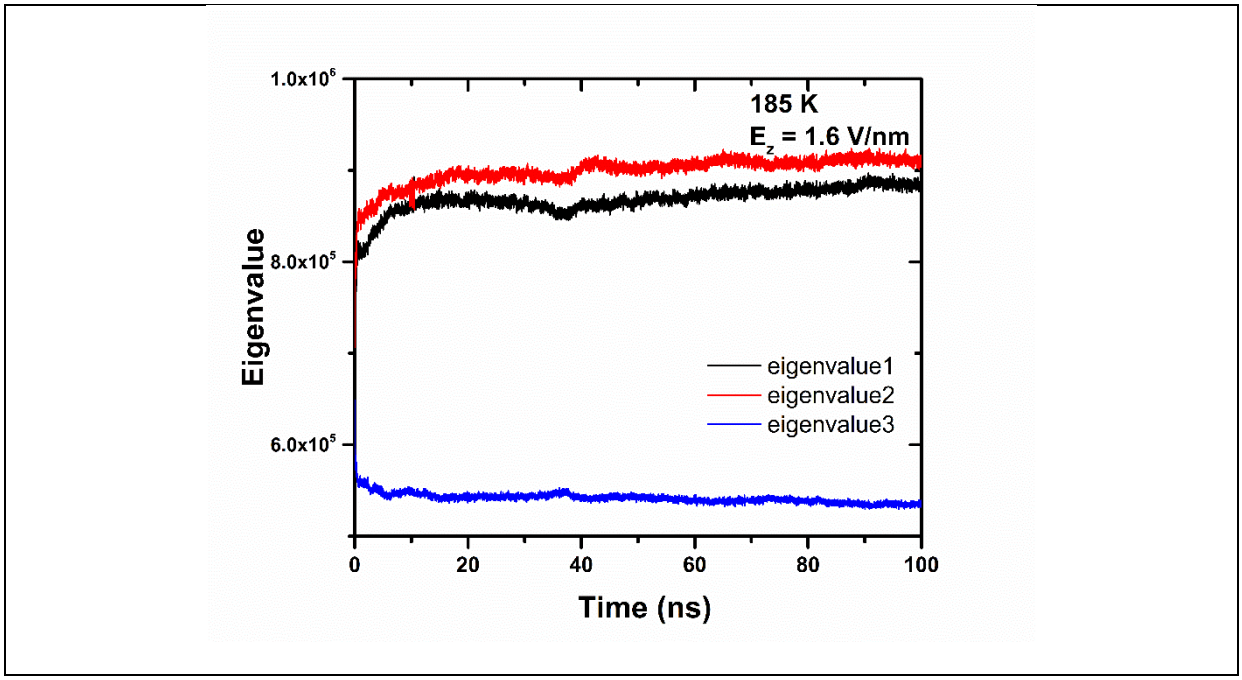

Figure S4. Eigenvalues of the moment-of-inertia tensor at each instant of time during electro-nucleation in a water droplet at 185 K subjected to an external static field of magnitude 1.6 V/nm along the laboratory *z*-axis. The eigenvalue along one of the principal axes (001) is substantially different from the other two mutually orthogonal axes; this implies an elongation of the resulting ice crystal along the external-field direction which coincides with the direction of this principal axis.

(f) View of the cross-sections of the ice crystal at 185 K subjected to 1.6 V/nm external field:

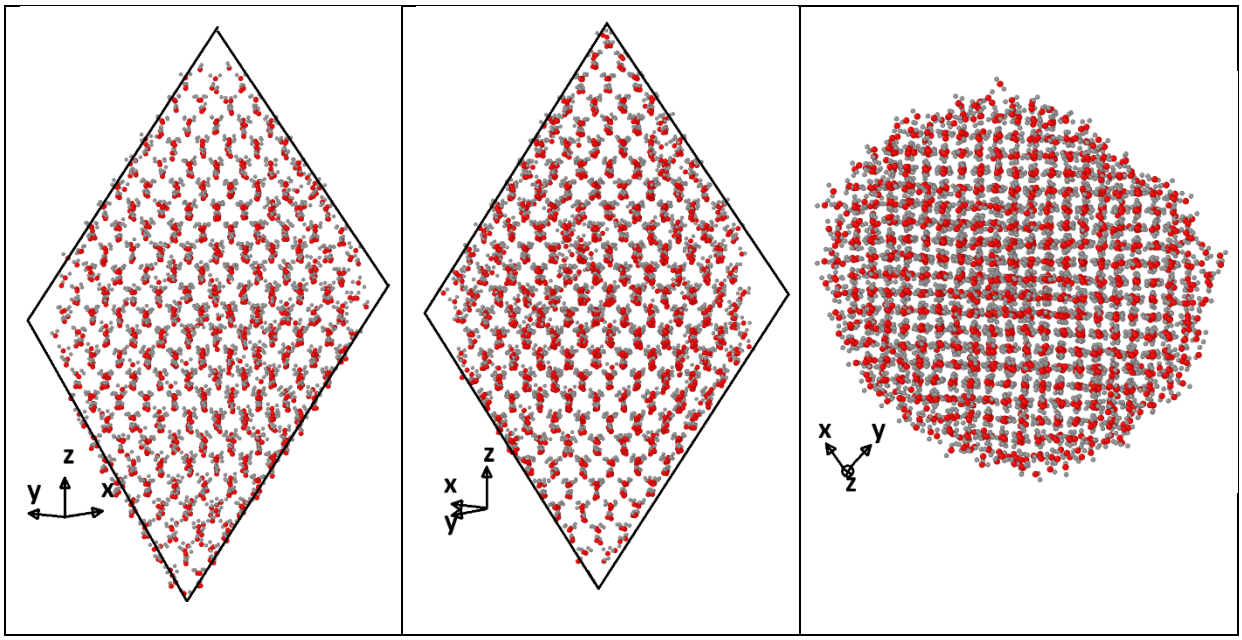

Figure S5. View of the cross-sections along the three principal axes of the electro-nucleated ice crystal at 185 K under a 1.6 V/nm static external field. The rhombus-shaped cross-sections resemble very loosely those of an octahedron, but, when viewed along the *z*-direction (the direction of the applied external field), it resembles a circle (see main text).

(g) Dipole alignment and proton ordering

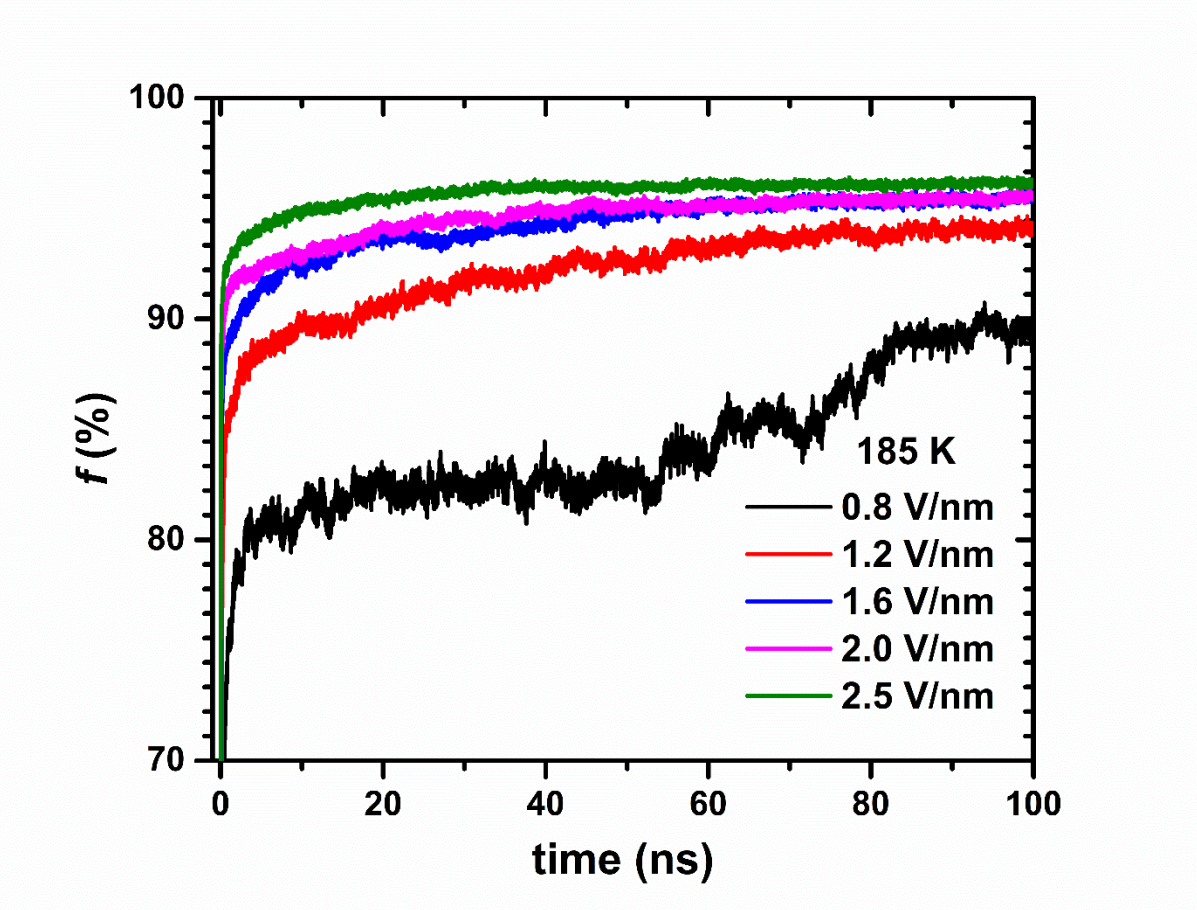

Figure S6. Temporal evolution of dipole alignment, characterising proton ordering, as a function of external field intensity at 185 K for fields of various intensity. The % alignment of the total system dipole (from the vector sum of individual molecular dipoles) along the laboratory *z*-axis is found relative to the theoretical level of full alignment of each and every water molecule's perfect dipole alignment along the *z*-axis.

(h) Cubicity and crystallinity measures

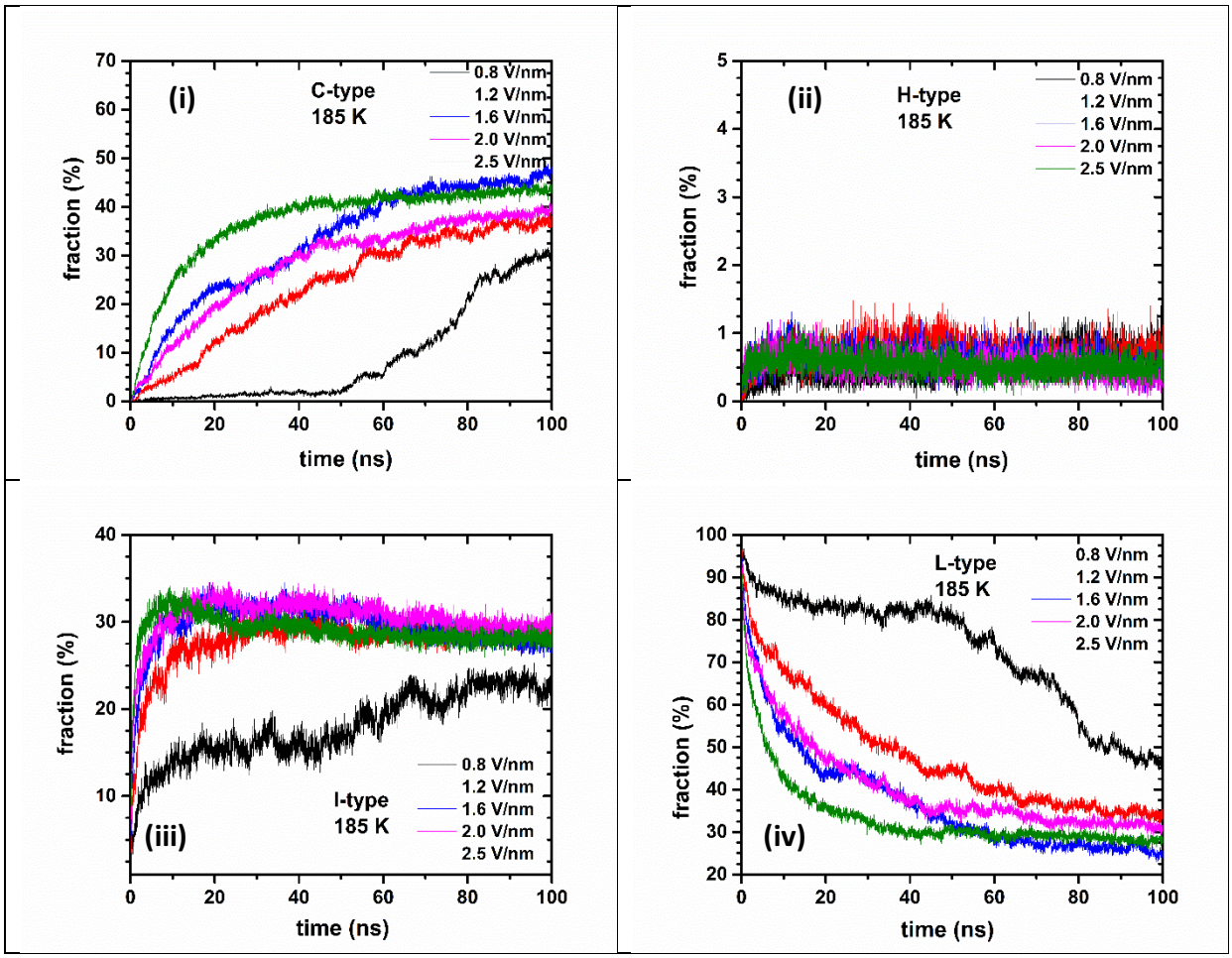

Figure S7. Temporal evolution of crystallinity/'cubicity' as a function of external field intensity at 185 K for fields of various intensity. The fraction of water molecules belonging to: (i) cubic ice, (ii) hexagonal ice, (iii) interfacial ice and (iv) liquid phase, as determined by the CHILL algorithm, are shown. The external field is applied along the laboratory *z*-axis. Clearly, the external field intensity plays a crucial role in determining the rate of crystallization: as intensity is lowered, the onset of crystallisation is delayed significantly.

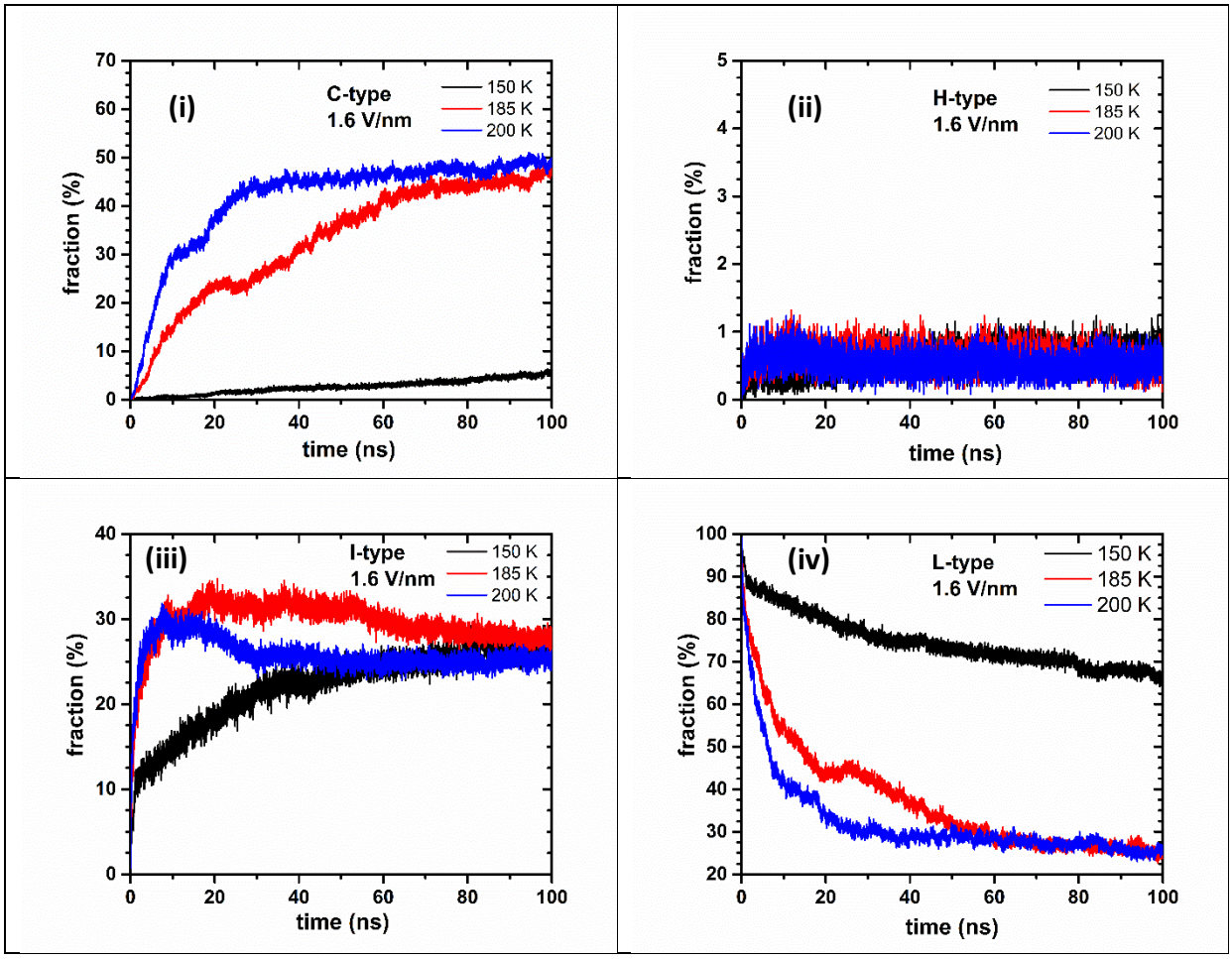

Figure S8. Temporal evolution of crystallinity/ 'cubicity' as a function of temperature at an external-field intensity of 1.6 V/nm along the laboratory *z*-axis. The fraction of water molecules belonging to: (i) cubic ice, (ii) hexagonal ice, (iii) interfacial ice and (iv) liquid phase, as determined by the CHILL algorithm, are shown. Temperature also plays a crucial role in determining the rate of crystallisation under the influence of external fields.

(i) Cubic- vs. Hexagonal- Ice RDF analysis

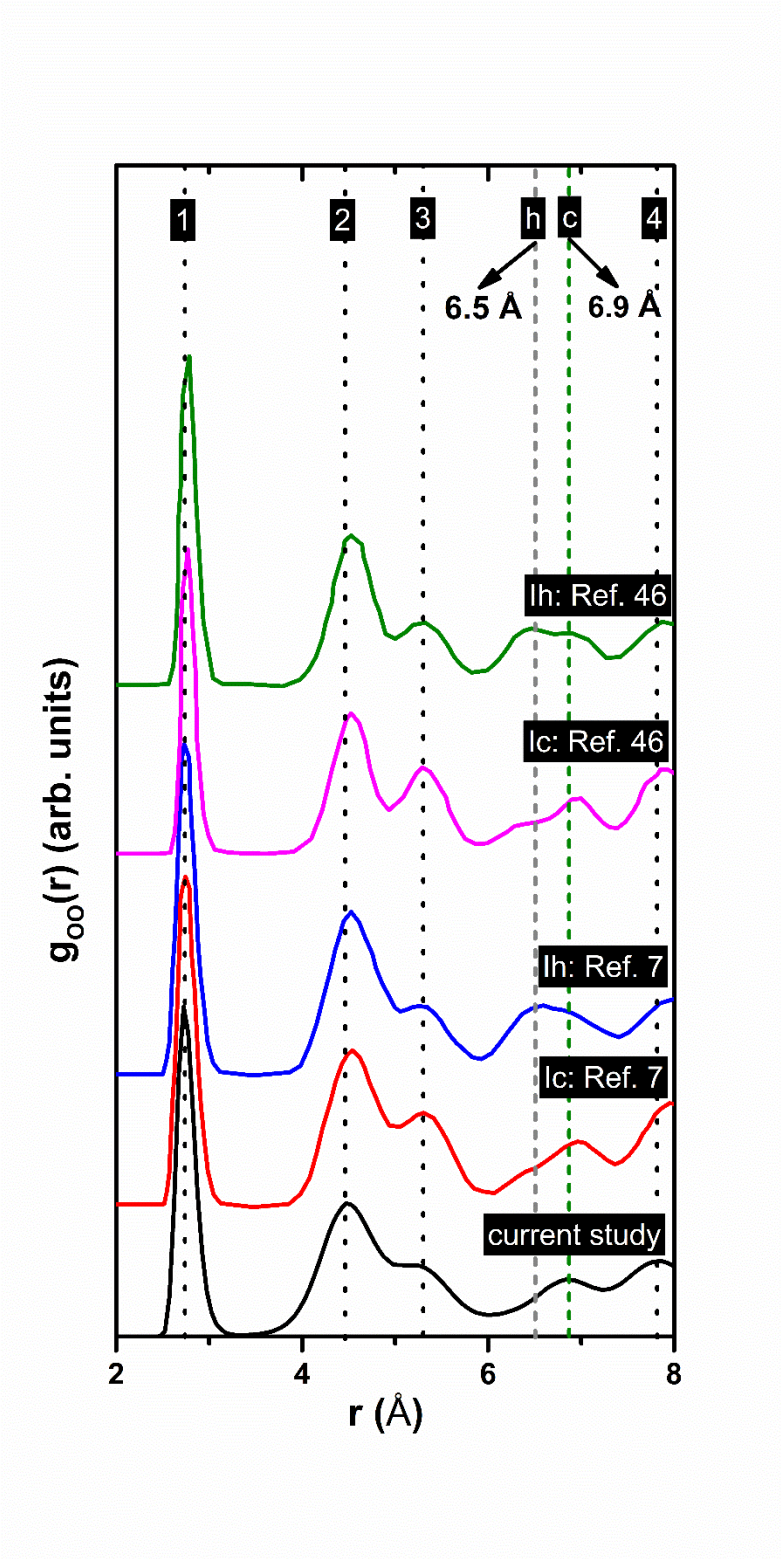

Figure S9: RDF plots from refs. 7 and 46 alongside those of the fully crystalline nano-droplet after 400 ns for the 185 K / 1.6 V/nm case. Peaks are marked as 1, 2 3, h, c and 4. The I_c and I_h RDFs are almost indistinguishable, except for the 'h' and 'c' peaks centred at ~6.5 and 6.9 Å, respectively. The essential conclusion is that the electro-nucleated is cubic (see main text). For ease of viewing, RDF plots are displaced vertically.

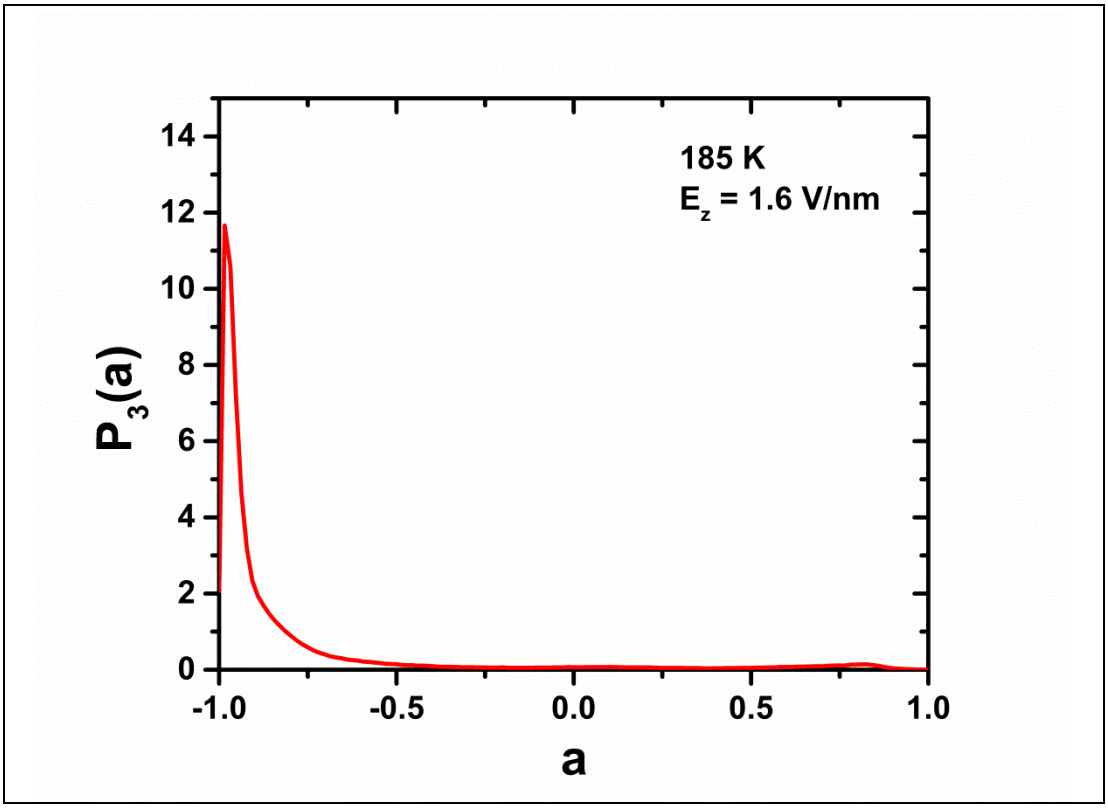

Figure S10. Plots showing the distribution of the alignment of local orientational structure, a, as defined by eqn. 5 of ref. 36, $a(i,j) = \frac{\widehat{q_l}(i).\widehat{q_l}(j)}{|\widehat{q_l}(i)|.|\widehat{q_l}(j)|}$, for l = 3. In this plot, we show the distribution for the water molecules in the nano-droplet at 185 K subjected to an external static electric field of magnitude 1.6 V/nm. This resembles the distribution for cubic ice (I_c), which further confirms the cubic crystalline phase of the electro-nucleated ice-crystal obtained in the present study.

(j) Stability of electro-frozen crystallite upon field removal at 185 K:

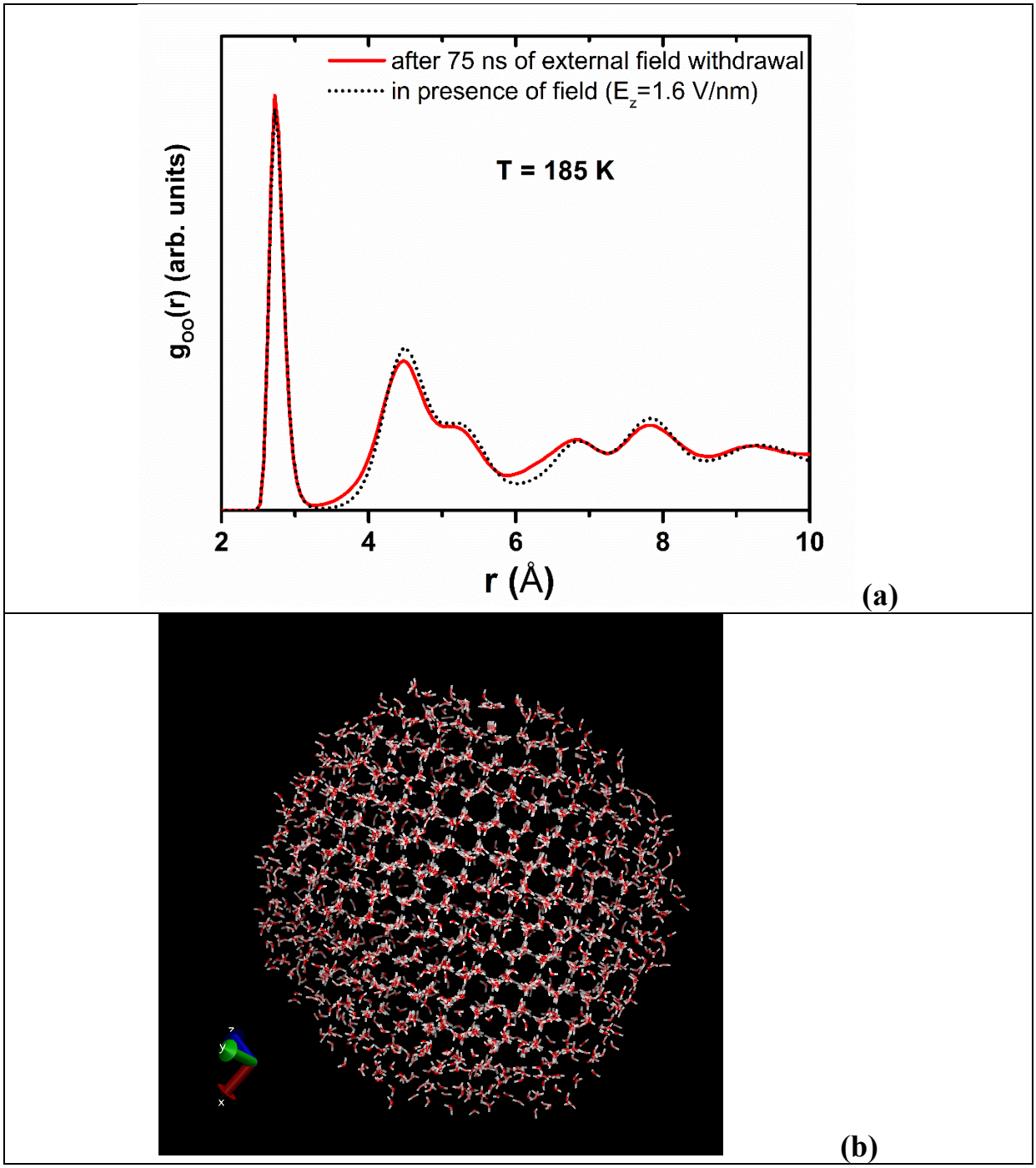

Figure S11. (a) Partial radial distribution function for the O-O pairs of the water nano-droplet at 75th nanosecond after the withdrawal of the external field, compared with the RDF of the ice crystallite obtained in the presence of an external field of magnitude 1.6 V/nm at 185 K (after electro-crystallisation). (b) The shape of the ice crystallite has lost the distinct octahedral shape after 75 ns, which was observed in presence of field; it becomes almost spherical in the absence of the external field.

(k) Additional details on simulation methodology:

All NE-MD simulations were performed using GROMACS[S2] under periodic boundary conditions with the TIP4P/2005 potential model for water.[S3] The system consists of a spherical water droplet of radius ~2.5 nm consisting of 2500 water molecules. The droplet was placed at the centre of a cubic periodic box of size 100 nm so that the interactions between its periodic images is essentially non-existent.

Each simulation run was carried out at constant temperature and constant volume. A Nosé-Hoover[S4] (NH) thermostat was applied to impose the desired system temperature with coupling constant 1 ps. Sudden cooling at the beginning of the simulation exhibits typical oscillatory behaviour of system temperature during a first few picoseconds. After this period, the system temperature oscillated around its prescribed value. We are aware that the initial oscillations are largely affected by the NH thermostat; however, the NH algorithm was chosen because it can reproduce canonical ensemble and its time-reversibility (in contrast to velocity scaling, weak coupling or stochastic approaches).

The system was propagated in time using the leap-frog MD integrator with time step of 3 fs. The relatively long time step was justified by constraining all bond lengths and angles in the system by a LINCS algorithm of fourth order.[S5] We updated the Verlet neighbour list every 10 steps, which we found sufficient by checking zero-field NVE dynamics, where no jumps in potential / total energies were observed, coupled with good energy conservation.

References

S2. Spoel, D. V. D.; Lindahl, E.; Hess, B.; Groenhof, G.; Mark, A. E.; Berendsen, H. J. C. GROMACS: Fast, flexible, and free. *J. Comput. Chem.* **2005**, 26, 1701-1718.

S3. Abascal, J. L. F.; Vega, C. A general purpose model for the condensed phases of water: TIP4p/2005. *J. Chem. Phys.* **2005**, *123*, 234505.

S4. Hoover, W. G. Canonical dynamics: Equilibrium phase-space distributions. *Phys. Rev. A* **1985**, 31, 1695-1697.

S5. Hess, B.; Bekker, H.; Berendsen, H. J. C.; Fraaije, J. G. E. M. LINCS: A linear constraint solver for molecular simulations. *J. Computational Chem.* **1997**, 18, 1463-1472.